THE JOURNAL OF PHYSICAL CHEMISTRY C

pubs.acs.org/JPCC Article

Potential Interaction of Noble Gas Atoms and Anionic Electrons in Ca_2N

Qin Qin, Biao Wan,* Bingmin Yan, Bo Gao, Qingyang Hu, Dongzhou Zhang, Hideo Hosono, and Huiyang Gou*

Cite This: *J. Phys. Chem. C* 2020, 124, 12213−12219

Read Online

ACCESS | Metrics & More | Article Recommendations

ABSTRACT: Noble gas (NG) is often used as a hydrostatic pressure-transmitting medium in high-pressure experiments. However, the NG atoms under compression are found to be readily trapped in the voids of some ionic compounds. Electrides usually have large open frameworks and show strong hydrogen and oxygen affinities. To investigate the interaction of light NG with electrides under pressure, we perform the structural investigations of Ca_2N in a diamond anvil cell under different NG (He, Ne, and Ar) conditions, assisted by density functional theory calculations. Experimental results find that in comparison with nonhydrostatic pressure, transition paths of Ca_2N change with different pressure media and phase transition pressure is reduced significantly, and NG is chemically inert for electrides in the studied pressure range. Theoretical analysis indicates that the anionic electrons in Ca_2N electride show strong repulsion with NG, preventing NG atoms from entering electrides. Such repulsion is due to the almost neutral character of noble atoms in electrides, which makes it difficult for them to interact with anionic electrons. Moreover, in the predicted metastable Ca_2N−NG, the neutral features of NG atoms result in the reservation of the intrinsic electride character. Our results reveal that the NGs can be used as protective gases for electrides under ambient conditions or hydrostatic pressure-transmitting media for the studies of high-pressure electrides within 50 GPa.

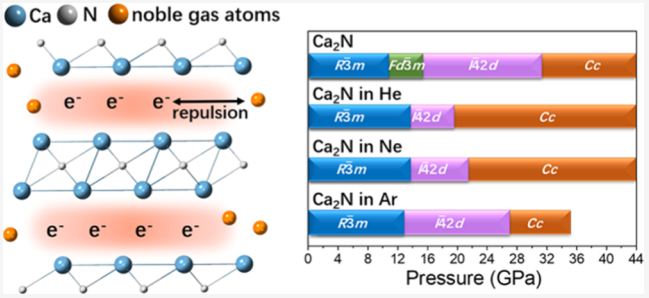

INTRODUCTION

The noble gases (NGs), helium, neon, and argon, are widely used in high-pressure science as hydrostatic pressure-transmitting media because of the highly inert character with closed shell.[1] NG is stable over a wide pressure range, which can generate hydrostatic pressure around the samples.[2−4] In high-pressure experiments, pressure-transmitting medium will change the behavior of the samples by weakening the nonhydrostatic effects (pressure gradients, shear stresses, and uneven pressure distributions) on the sample.[5] Different pressure-transmitting media may lead to the varied structural evolutions under pressure.[6] Nevertheless, in some cases, NGs such as argon,[7] neon,[8] and helium[9] can be trapped under pressure as guest atoms within the compounds especially with sizable voids. Large voids usually destabilize materials under high pressure; however, the intercalation of NG may help to maintain the structure integrity under compression.[10,11] Mixing helium with ionic alkali oxide,[10,12] sulphide,[12] and alkaline earth fluorides[13] are even predicted to produce stable compounds at high pressure. Notably, theoretical analysis[13,14] reveals that NGs (He and Ne) have the propensity to react with a variety of ionic compounds at pressure as low as 30 GPa. Recent calculations suggest that the helium atom inserts into the ionic compounds containing an unequal number of cations and anions at close to ambient pressure.[15,16] The formed phases are bound by van der Waals forces, and the framework with NG atoms is electron neutral.

Electride is a unique class of ionic compound in which excess electrons are trapped in the interstitial voids and serve as anion electrons (AEs).[17] These AEs do not belong to any particular atoms or molecules but are loosely bound in the crystal lattices. The intrinsic electronic properties in electrides exhibit many exotic properties such as low work function and high electronic mobility.[18] Depending on the host electride, AEs are trapped in the cage-like vacancies of zero-dimensional (0D) materials (e.g., C12A7,[19] Ti_2O,[20] and Li_4N[21]) or the channel-like voids of one-dimensional (1D) structures (e.g., Li_3O,[22] Y_2Cl_3,[23] and Y_5Si_3[24]), or the interstitial spaces of two-dimensional (2D) layers (e.g., Ca_2N,[18] Y_2C,[25] and YCl[23]),

Received: February 22, 2020
Revised: April 12, 2020
Published: May 1, 2020

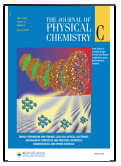

https://dx.doi.org/10.1021/acs.jpcc.0c01543
J. Phys. Chem. C 2020, 124, 12213−12219

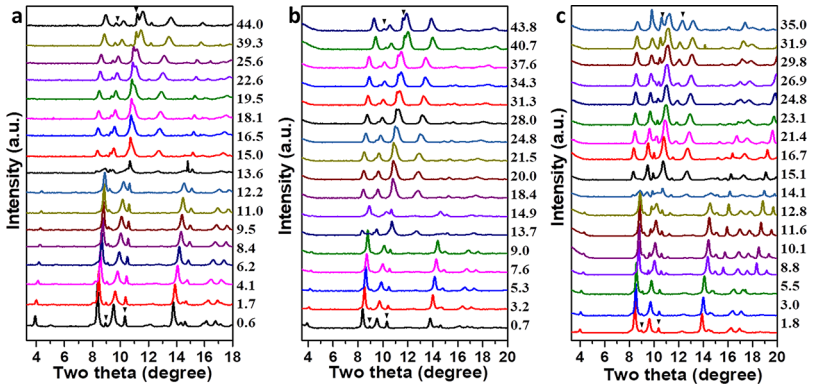

Figure 1. Obtained XRD patterns for Ca_2N at high pressure with (a) helium, (b) neon, and (c) argon. Quite a small amount of CaO impurity is traced by the black inverted triangles, which does not affect the observed phase changes.

respectively. Because of its loosely packed but strongly interacted ionic structure, an ambient stable electride is still under investigation. Therefore, imposing external high pressure becomes a general method in exploring novel electrides. Many high-pressure electrides have been predicted, such as Li_6P,[26] Sr_5P_3,[27] and Sr_3CrN_3.[28] AEs can easily transfer electrons to other atoms or molecules, such as hydrogen, oxygen, and water. NG atoms with higher electronegativity can attract electrons easily. Mg is found to form stable electrides with Xe, Kr, and Ar above 125, 250, and 250 GPa, respectively.[29] In Mg−Xe compounds, Xe gains electrons and becomes highly negatively charged (−1.03 e in Mg_2Xe at 50 GPa). The formation pressure of electrides in Mg−NG is lower than pure Mg, which is predicted to be above 500 GPa.[30] Lighter NG atoms also change the formation pressure of electride. For example, Na reacts with He under 113 GPa to form Na_2He electrides,[31] and the formation of pure Na electride occurs under ∼200 GPa.[13] Moreover, He atoms are far away from the anionic electrons and are almost electron neutral (−0.151 e). Thus, the interaction mechanism between AEs and lighter NGs remains elusive. We are motivated to develop a comprehensive understanding of the interaction between lighter NG atoms and the AEs.

In order to explore the effect of different NGs on the formation of high-pressure electrides, we perform *in situ* high-pressure X-ray diffraction (HPXRD) coupled with density functional theory (DFT) calculations to study the phase transitions of Ca_2N in different NG (He, Ne, and Ar) media in the classic 2D electride dicalcium nitride (Ca_2N). Ca_2N has a large interlayer spacing of about 4 Å,[18] which is stacked along its *c*-axis. The interlayer region between cation $[Ca_2N]^+$ layers acts as the anion activity region. From ambient pressure to 50 GPa, Ca_2N undergoes multiple structural transformations, and the transformed structures are all electrides. In this work, we study the effect of pressure-transmitting media on the phase transitions of Ca_2N within 50 GPa and analyze the interaction with NGs under pressure.

METHODS

Experimental Methods. The synthesis of polycrystalline Ca_2N can be found in previous studies.[18,32] A symmetrical diamond anvil cell (DAC) with a pair of 300 μm culets was used in this study. The sample chamber is a hole of ∼150 μm in diameter, which is drilled in stainless steel gasket by laser drilling. Ca_2N powder, ruby balls, and He, Ne, and Ar as gas media were loaded into the sample chamber using a high-pressure gas-loading system.[33] All the loading process was performed in an argon-filled glovebox to prevent the degradation of Ca_2N in air. The *in situ* synchrotron HPXRD measurements were conducted at beamline of 13-BM-C, Advanced Photon Source. HPXRD patterns were collected with an X-ray wavelength of 0.4337 Å. The 2D diffraction images were integrated into 1D pattern with the Dioptas program.[34] Structural information of Ca_2N was obtained using GSAS + EXPGUI software packages.[35]

Computational Details. The variable and fixed composition searches for Ca_2N−He, Ca_2N−Ne, and Ca_2N−Ar were performed using USPEX[36] and CALYPSO[37,38] codes. During the structural searching, the pressure was set as 50 and 100 GPa, and the ratio of Ca and N was fixed at 2. The total number of atoms of the generated structures is up to 40. Structure relaxations and electronic structure calculations were performed using the Vienna Ab initio Simulation Package.[39] The generalized-gradient approximation with the Perdew−Burke−Ernzerhof functional[40] was employed to treat the electron exchange−correlation interactions. The PAW potentials with valence electrons of Ca: $3p^6$, $4s^1$, $3d^{0.01}$; N: $2s^2$, $2p^3$; and He: $1s^2$ were used. The positively charged Ca_2N and Ca_2NHe were built through decreasing the total number of electrons. To ensure the enthalpy calculations, tensors and stress are well converged, the plane-wave kinetic energy cutoff was set as 600 eV, and the Brillouin zone was sampled with a resolution of $2\pi \times 0.03$ Å^{-1}.

RESULTS AND DISCUSSION

To study the effect of NG on the structure evolutions of Ca_2N under pressure, Ca_2N powder and NGs (helium, neon, and argon) are loaded into DAC to perform *in situ* synchrotron HPXRD measurements. HPXRD measurements reveal that NG elements do not form stable compounds with Ca_2N under pressure below 50 GPa. It is worth noting that helium, neon, and argon solidify at about 12.1, 4.8, and 1.5 GPa at ambient temperature,[41,42] respectively. Even after solidification, they are soft enough to release stress and maintain excellent hydrostatic condition under pressure below 50 GPa. Obtained XRD patterns of Ca_2N with different pressure media are shown in Figure 1. Their phase transition sequences under pressure are identified by resolving powder XRD patterns with Rietveld analysis.

In He pressure media, diffraction peaks are initially indexed in the anti-$CdCl_2$ structure with $R\bar{3}m$ symmetry (space group no. 166). As the compression continues above 13.6 GPa in

https://dx.doi.org/10.1021/acs.jpcc.0c01543
J. Phys. Chem. C 2020, 124, 12213−12219

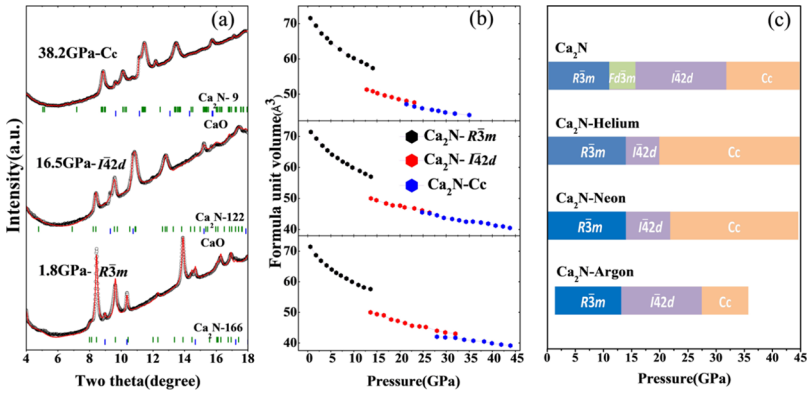

Figure 2. (a) Rietveld refinements of XRD patterns of Ca_2N under pressure in helium; (b) volume pressure dependence of Ca_2N (upper panel: helium, middle panel: neon, lower panel: argon). Red lines indicate the fitted patterns, the green tick marks show the Bragg reflections of Ca_2N with the $R\bar{3}m$ structure, $I\bar{4}2d$ structure, and Cc structure, blue tick marks for the CaO phase; (c) pressure range of Ca_2N phase transition and the phase transition paths with different pressure-transmitting media. Blue bar is the pressure range with the $R\bar{3}m$ phase, green bar for the $Fd\bar{3}m$ phase, and purple and yellow color bars for the $I\bar{4}2d$ and Cc phases.

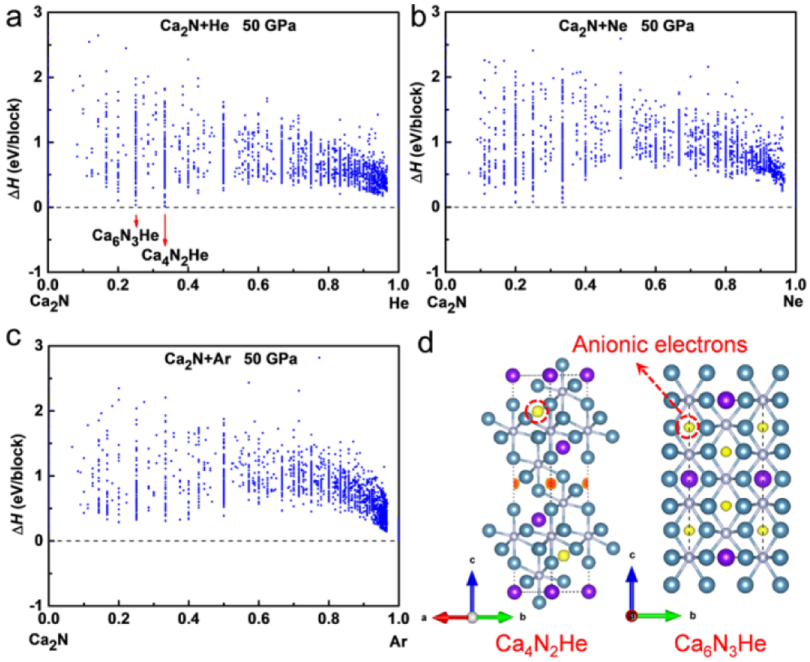

Figure 3. Calculated convex hulls for the (a) Ca_2N−He, (b) Ca_2N−Ne, and (c) Ca_2N−Ar systems at 50 GPa. (d) ELFs for Ca_4N_2He and Ca_6N_3He.

helium, Ca_2N matches with the tetragonal $I\bar{4}2d$-type structure. With continued compression, the intensity of the second strongest peak at 16.5 GPa gradually weakened, and the (202) peak at $2\theta \approx 9.5°$ becomes the fourth strongest peak at 19.5 GPa (Figure 1a). This change indicates that the transition from $I\bar{4}2d$-type structure to the Cc phase starts and completes at about 22.6 GPa. The two phases coexist for about 3 GPa. Such a phenomenon is also observed in Ca_2N using neon and argon as pressure media. In neon, the diffraction pattern of $R\bar{3}m$ changes gradually at 13.7 GPa, $I\bar{4}2d$ structure started to transform into a Cc structure at 21.5 GPa, and the transformations completed at ∼23 GPa (Figure 1b). In Ar (Figure 1c), when the pressure increases to 12.8 GPa, $R\bar{3}m$ structure transforms into the $I\bar{4}2d$ structure. The $I\bar{4}2d$-type structure starts to transform into the Cc phase at 26.9 GPa, and the transformation completes at ∼ 28 GPa. All the peaks are indexed in $R\bar{3}m$ at modest pressure, and then, the samples transform into the $I\bar{4}2d$ structure (space group no. 122) under pressure. However, the $Fd\bar{3}m$ structure observed previously without pressure medium is barely seen in Ca_2N under NG media. The difference in the transition pressure comes from the hydrostatic condition.[43]

The detailed structural information including lattice parameters and volumes from Rietveld refinements in helium are shown in Figure 2. Here, we mainly discuss the results of Ca_2N in helium because of the similarity of the structural transitions of Ca_2N in helium, neon, and argon. The results of neon and argon media are also obtained. The hR3 phase with $R\bar{3}m$ symmetry features 2D Ca_2N layers with a large interlayer spacing (∼4 Å) along the c-axis. The $R\bar{3}m$ structure consisted of Ca_2N slabs formed by an edge-shared Ca_6 octahedron, each Ca atom is connected to three N atoms with the coordinates of Ca (0, 0, $\pm u$) and N (0,0,0) in the rhombohedral units. From the Rietveld refinement of the $R\bar{3}m$ phase, the compression of

https://dx.doi.org/10.1021/acs.jpcc.0c01543
J. Phys. Chem. C 2020, 124, 12213−12219

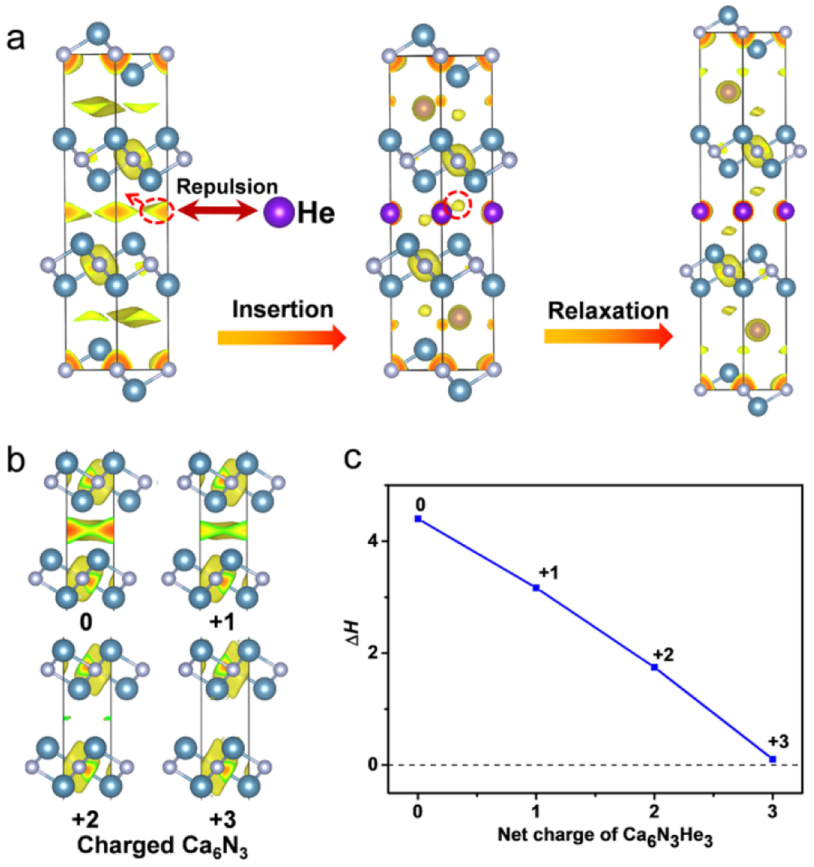

Figure 4. ELFs for Ca_2N (left), Ca_4N_2He (before relaxation, middle), and Ca_6N_3He (after relaxation, right). (b) ELFs for Ca_6N_3 with different charge conditions. (c) Formation enthalpies for charged $Ca_6N_3He_3$ relative to He and charged Ca_2N.

the *a*-axis of Ca_2N with different gases is relatively unaffected. The obtained lattice parameters show that the *c*-axis changes rapidly (a = 3.59 Å, c = 18.69 Å, at 1.8 GPa, as shown in Figure 2a). At higher pressure, anti-$CdCl_2$-structured Ca_2N transforms into the $I\bar{4}2d$ structure with the lattice parameters of a = 7.21 Å and c = 7.50 Å at 16.5 GPa. Ca_2N transformed into the Cc structure with the lattice parameters of a = 6.87 Å, b = 9.83 Å, c = 5.87 Å, and β = 124.1° at 38.2 GPa. The similarity between the monoclinic Cc structure and $I\bar{4}2d$ can be seen from the simulated XRD patterns. In addition, the Cc structure is closely related to the $I\bar{4}2d$ structure through a lattice distortion with β angles changing from 90 to 124.1°. The pressure dependence of Ca_2N molar volume follows a smooth, concave curve, as seen in Figure 2b. The transition from $R\bar{3}m$-type to the $I\bar{4}2d$-type structure is accompanied with an obvious volume collapse of 13.3% in helium, which is different from 12.6% in neon and 13.6% in argon. The pressure-dependent unit-cell volumes can be fitted by the third-order Birch–Murnaghan equation of state.[44] The bulk modulus of B_0 = 44.6 ± 0.9 GPa under ambient pressure, the pressure derivative of B_0' = 2.6 ± 0.1, and volume of V_0 = 71.5 ± 0.1 Å^3 for $R\bar{3}m$ symmetry in helium under ambient pressure was observed. B_0 = 41.0 ± 3.4 GPa, B_0' = 3.5 ± 0.5, and V_0 = 71.5 ± 0.3 Å^3 for $R\bar{3}m$ symmetry in neon and B_0 = 42.3 ± 2.5 GPa, B_0' = 3.3 ± 0.4, and V_0 = 71.6 ± 0.2 Å^3 for $R\bar{3}m$ symmetry in argon were observed.

The phase transition pressures of Ca_2N under hydrostatic conditions are lower than those under nonhydrostatic conditions, and the phase transition path is changed as well (Figure 2c). The space group of Ca_2N evolves from $R\bar{3}m$ (0–11.2 GPa) to $Fd\bar{3}m$ structure (11.2–14.6 GPa), then to $I\bar{4}2d$(14.6–29.4 GPa) and finally completes with the Cc phase mentioned above 29.4 GPa during compression without medium. However, by comparing the different XRD patterns with Rietveld analysis, it is found that the $R\bar{3}m$ phase is present at almost the same pressure range, while the obvious disparity is found at $I\bar{4}2d$ phase pressure range. The majority of $R\bar{3}m$ phase transforms into the $I\bar{4}2d$ phase near 14 GPa. At about 15 GPa, $R\bar{3}m$ phase disappears. Meanwhile, the volume accelerates to decrease with increasing pressure. The $I\bar{4}2d$-type structure starts to transform into Cc and completes at different pressures in different media. A high-pressure Cc phase (space group no. 9) shows up at 19.5 GPa with pressure medium of helium, 21.5 and 26.9 GPa with neon and argon, respectively.

To further investigate the interactions of Ca_2N and NG, we carry out variable-structure searches for Ca_2N–NG. The convex hulls are constructed for Ca_2N–He (Figure 3a), Ca_2N–Ne (Figure 3b), and Ca_2N–Ar (Figure 3c) using the generated structures in variable-composition structure search at 50 GPa. All generated compounds of Ca_2N–He, Ca_2N–Ne, and Ca_2N–Ar show positive formation enthalpies, suggesting that they are thermodynamically unstable. Moreover, NG with greater atomic radii possesses higher positive formation enthalpies, which usually occupies larger interstitial voids. The *PV* term (enthalpies $H = U + PV$) contributes to the pressure-induced stability of NG containing compounds (e.g., A_2S–NG and A_2O–NG).[10] NG atoms with big atomic radii possess higher formation enthalpies under pressure.[10] In our previous investigation,[32] Ca_2N transforms into 0D electride

https://dx.doi.org/10.1021/acs.jpcc.0c01543
J. Phys. Chem. C 2020, 124, 12213–12219

under 50 GPa. We fully relax the energetically competitive phases of Ca_4N_2He and Ca_6N_3He and calculate their electron localization function (ELF)[45,46] (Figure 4d). Highly localized ELF_{max} off the nuclei can be observed in Ca_4N_2He and Ca_6N_3He, suggesting that the insertion of NGs show less effects on the intrinsic electride characters of Ca_2N. He atoms are surrounded by Ca and N atoms, which is far away from anionic electrons. Calculated Bader net charge for He in Ca_6N_3He and Ca_4N_2He is −0.099 and −0.090 e, respectively, supporting the chemical inertness character of He atoms in Ca_2N.

In contrast to the previously reported A_2B−NG compounds,[13] Ca_2N−NG compounds are only metastable. To uncover the origin of instability in Ca_2N−NG, we manipulate the Ca_2NHe structure by inserting He atoms into the position of anionic electrons. ELF is calculated for Ca_2N and Ca_2NHe (Ca_6N_3He here) before and after structure relaxation. Ca_2N is 2D electride with ELF_{max} located at the center of Ca_6 octahedron. It was reported that H atoms tend to insert into the Ca_6 octahedron,[47] which resulted in the transfer of anionic electrons into the H 1s orbitals. Such a phenomenon is not observed when He is inserted into the position of anionic electrons in Ca_2N. ELF maps suggest strong repulsion between He atoms and anionic electrons. The insertion of He atoms induces the reconstruction of AE charge densities, which shift to the interstitial voids consisting of He and Ca atoms. Previously,[48] only the "stable voids" comprised by same elements can host anionic electrons. However, the anionic electrons in Ca_2NHe are observed in the voids surrounded by Ca and He atoms. Using Bader net charge analysis, He atom is almost neutral with the net charge of −0.15 e. The interaction between the NG atoms and the host oxide/sulfide is rather weak, He atoms can thus serve as a component with other atoms to form "stable voids." Similar characters are also reported in heavier NG contend Mg−NG (NG = Xe, Kr and Ar) compounds,[29] whose interstitial voids consisted of Mg and NG atoms. Such a phenomenon is essential for the design of novel high-pressure electrides. In A_2O−NG and A_2S−NG compounds,[12] the volumes of A_2O and A_2S are almost not changed after the insertion of NG atoms. When the structure of $Ca_6N_3He_3$ is fully relaxed, the *c* axis expands significantly because of the strong repulsion between He and anionic electrons. To provide further insights into the He−AE interaction, we calculate the formation enthalpy of $Ca_6N_3He_3$. The total electrons in Ca_2N and Ca_2NHe are modified to reduce the magnitude of anionic electrons. In positively charged Ca_2N (Ca_6N_3 here), the magnitude of anionic electrons in Ca_2N decreases and finally disappears with the net charge of Ca_2N increasing from 0 to +3. With the decrease of magnitude of anionic electrons, the formation enthalpy of $Ca_6N_3He_3$ is also lowered significantly (Figure 4c). The repulsion between He and anionic electrons is responsible for the instability of Ca_2N−He compounds.

The repulsion between NG and anionic electrons suggests that the large interstitial voids (occupied by anionic electrons) in electrides cannot help in capturing light NG atoms both under ambient and high pressure conditions. Considering that Ca_4N_2He and Ca_6N_3He are slightly above the convex hull, thus light NG may form stable compounds with other electrides under higher pressure, for example, Na_2He is stable above 200 GPa.[31]

CONCLUSIONS

Using *in situ* HPXRD and DFT calculations, we investigate the effects of light NGs (He, Ne, and Ar) on the formation of high-pressure Ca_2N electrides. The interactions between anionic electrons and NGs atoms are also discussed. Both experimental and calculation results support the conclusion that light NG atoms are chemically inert for Ca_2N electrides, suggesting that the light NGs are good pressure-transmitting media for high-pressure electrides. The hydrostatics of different NGs changes the transition path and alters their phase transition pressures. In the Ca_2N−NG compounds, the NG atoms are almost electron neutral and show a strong repulsion with the NG atoms, thereby preventing NG atoms from entering into electrides. Moreover, in the hypothetical Ca_2N−NG compounds, the existence of NG atoms have a minor influence on the intrinsic electride characteristics of Ca_2N both under ambient and high pressure conditions, which indicates that NG atoms can be used to find novel electrides.

AUTHOR INFORMATION

Corresponding Authors

Biao Wan − *Center for High Pressure Science and Technology Advanced Research, Beijing 100094, China*; Email: wan.biao@hpstar.ac.cn

Huiyang Gou − *Center for High Pressure Science and Technology Advanced Research, Beijing 100094, China; Key Laboratory of Applied Chemistry, College of Environmental and Chemical Engineering, Yanshan University, Qinhuangdao 066004, China*; orcid.org/0000-0002-2612-4314; Email: huiyang.gou@hpstar.ac.cn

Authors

Qin Qin − *Center for High Pressure Science and Technology Advanced Research, Beijing 100094, China*

Bingmin Yan − *Center for High Pressure Science and Technology Advanced Research, Beijing 100094, China*

Bo Gao − *Center for High Pressure Science and Technology Advanced Research, Beijing 100094, China*

Qingyang Hu − *Center for High Pressure Science and Technology Advanced Research, Beijing 100094, China*; orcid.org/0000-0002-2742-3017

Dongzhou Zhang − *Hawai'i Institute of Geophysics and Planetology, School of Ocean and Earth Science and Technology, University of Hawai'i at Manoa, Honolulu, Hawaii 96822, United States*

Hideo Hosono − *Materials Research Center for Element Strategy and Laboratory for Materials and Structures, Institute of Innovative Research, Tokyo Institute of Technology, Yokohama, Kanagawa 226-8503, Japan*; orcid.org/0000-0001-9260-6728

Complete contact information is available at: https://pubs.acs.org/10.1021/acs.jpcc.0c01543

Notes

The authors declare no competing financial interest.

ACKNOWLEDGMENTS

This project was supported from the National Natural Science Foundation of China (NSFC) under grant no. U1530402. This work was also supported from the MEXT Element Strategy Initiative, MEXT Kakenhi (no. 17H06153) and JST ACCEL Project. Portions of this work were performed at Geo-

SoilEnviroCARS, Advanced Photon Source, Argonne National Laboratory. Q. H. is supported from the National Natural Science Foundation of China (no. 17N1051-0213). GeoSoilEnviroCARS was supported from the National Science Foundation-Earth Sciences (EAR-1634415) and Department of Energy—GeoSciences (DE-FG02-94ER14466). This research used resources of the Advanced Photon Source, a U.S. Department of Energy (DOE) Office of Science User Facility operated for the DOE Office of Science by Argonne National Laboratory under contract no. DE-AC02-06CH11357. 13-BM-C operation was supported from the COMPRES through the Partnership for Extreme Crystallography (PX2) project under NSF Cooperative Agreement no. EAR 1661511. We also thank Sergey Tkachev at GSECARS for gas-loading.

REFERENCES

(1) Häussinger, P.; Glatthaar, R.; Rhode, W.; Kick, H.; Benkmann, C.; Weber, J.; Wunschel, H. J.; Stenke, V.; Leicht, E.; Stenger, H. *Noble Gases. Ullmann's Encycl. Ind. Chem.*; Wiley-VCH Verlag GmbH & Co. KGaA, 2001.

(2) Shen, G.; Mei, Q.; Prakapenka, V. B.; Lazor, P.; Sinogeikin, S.; Meng, Y.; Park, C. Effect of Helium on Structure and Compression Behavior of SiO_2 Glass. *Proc. Natl. Acad. Sci. U.S.A.* **2011**, *108*, 6004–6007.

(3) Celeste, A.; Borondics, F.; Capitani, F. Hydrostaticity of Pressure-Transmitting Media for High Pressure Infrared Spectroscopy. *High Pressure Res.* **2019**, *39*, 608–618.

(4) Kurnosov, A.; Kantor, I.; Boffa-Ballaran, T.; Lindhardt, S.; Dubrovinsky, L.; Kuznetsov, A.; Zehnder, B. H. A Novel Gas-Loading System for Mechanically Closing of Various Types of Diamond Anvil Cells. *Rev. Sci. Instrum.* **2008**, *79*, 045110.

(5) Shen, Y.; Kumar, R. S.; Pravica, M.; Nicol, M. F. Characteristics of Silicone Fluid as a Pressure Transmitting Medium in Diamond Anvil Cells. *Rev. Sci. Instrum.* **2004**, *75*, 4450–4454.

(6) Takemura, K.; Dewaele, A. Isothermal Equation of State for Gold with a He-Pressure Medium. *Phys. Rev. B: Condens. Matter Mater. Phys.* **2008**, *78*, 104119.

(7) Itoh, H.; Tse, J. S.; Kawamura, K. The Structure and Dynamics of Doubly Occupied Ar Hydrate. *J. Chem. Phys.* **2001**, *115*, 9414–9420.

(8) Yu, X.; Zhu, J.; Du, S.; Xu, H.; Vogel, S. C.; Han, J.; Germann, T. C.; Zhang, J.; Jin, C.; Francisco, J. S.; et al. Crystal Structure and Encapsulation Dynamics of Ice II-structured Neon Hydrate. *Proc. Natl. Acad. Sci. U.S.A.* **2014**, *111*, 10456–10461.

(9) Londono, D.; Kuhs, W. F.; Finney, J. L. Enclathration of Helium in Ice II: The First Helium Hydrate. *Nature* **1988**, *332*, 141–142.

(10) Gao, H.; Sun, J.; Pickard, C. J.; Needs, R. J. Prediction of Pressure-Induced Stabilization of Noble-Gas-Atom Compounds with Alkali Oxides and Alkali Sulfides. *Phys. Rev. Mater.* **2019**, *3*, 015002.

(11) Albert, V. V.; Sabin, J. R.; Harris, F. E. Simulated Structure and Energetics of Endohedral Complexes of Noble Gas Atoms in Buckminsterfullerene. *Int. J. Quantum Chem.* **2007**, *107*, 3061–3066.

(12) Sun, J.; Pickard, C. J.; Needs, R. J. Formation of Noble Gas Compounds with Alkali Oxides and Sulfides under Pressure. https://arxiv.org/abs/1409.2227/ (accessed Sept 9, 2014).

(13) Liu, Z.; Botana, J.; Hermann, A.; Valdez, S.; Zurek, E.; Yan, D.; Lin, H. Q.; Miao, M. S. Reactivity of He with Ionic Compounds under High Pressure. *Nat. Commun.* **2018**, *9*, 951.

(14) Hirai, H.; Uchihara, Y.; Nishimura, Y.; Kawamura, T.; Yamamoto, Y.; Yagi, T. Structural Changes of Argon Hydrate under High Pressure. *J. Phys. Chem. B* **2002**, *106*, 11089–11092.

(15) Liu, L.; Wang, C.; Yi, S.; Kim, D. K.; Park, C. H.; Cho, J. H. Theoretical Prediction of Weyl Fermions in the Paramagnetic Electride Y_2C. *Phys. Rev. B: Condens. Matter Mater. Phys.* **2019**, *99*, 220401.

(16) Wang, D.; Li, H.; Zhang, L.; Sun, Z.; Han, D.; Niu, L.; Zhong, X.; Qu, X.; Yang, L. First- Principles Study on OH-Functionalized 2D Electrides: Ca_2NOH and $Y_2C(OH)_2$, Promising Two-Dimensional Monolayers for Metal-Ion Batteries. *Appl. Surf. Sci.* **2019**, *478*, 459–464.

(17) Dye, J. L. CHEMISTRY: Electrons as Anions. *Science* **2003**, *301*, 607–608.

(18) Lee, K.; Kim, S. W.; Toda, Y.; Matsuishi, S.; Hosono, H. Dicalcium Nitride as a Two-Dimensional Electride with an Anionic Electron Layer. *Nature* **2013**, *494*, 336–340.

(19) Kim, S. W.; Shimoyama, T.; Hosono, H. Solvated Electrons in High-Temperature Melts and Glasses of the Room-Temperature Stable Electride $[Ca_{24}Al_{28}O_{64}]^{4+} \cdot 4e^-$. *Science* **2011**, *333*, 71–74.

(20) Zhong, X.; Xu, M.; Yang, L.; Qu, X.; Yang, L.; Zhang, M.; Liu, H.; Ma, Y. Predicting the Structure and Stability of Titanium Oxide Electrides. *npj Comput. Mater.* **2018**, *4*, 70.

(21) Tsuji, Y.; Dasari, P. L. V. K.; Elatresh, S. F.; Hoffmann, R.; Ashcroft, N. W. Structural Diversity and Electron Confinement in Li_4N: Potential for 0-D, 2-D, and 3-D Electrides. *J. Am. Chem. Soc.* **2016**, *138*, 14108–14120.

(22) Fang, H.; Zhou, J.; Jena, P. Super-Alkalis as Building Blocks of One-Dimensional Hierarchical Electrides. *Nanoscale* **2018**, *10*, 22963–22969.

(23) Wan, B.; Lu, Y.; Xiao, Z.; Muraba, Y.; Kim, J.; Huang, D.; Wu, L.; Gou, H.; Zhang, J.; Gao, F. Identifying Quasi-2D and 1D Electrides in Yttrium and Scandium Chlorides Via Geometrical Identification. *npj Comput. Mater.* **2018**, *4*, 77.

(24) Lu, Y.; Li, J.; Tada, T.; Toda, Y.; Ueda, S.; Yokoyama, T.; Kitano, M.; Hosono, H. Water Durable Electride Y_5Si_3: Electronic Structure and Catalytic Activity for Ammonia Synthesis. *J. Am. Chem. Soc.* **2016**, *138*, 3970–3973.

(25) Zhang, X.; Xiao, Z.; Lei, H.; Toda, Y.; Matsuishi, S.; Kamiya, T.; Ueda, S.; Hosono, H. Two-Dimensional Transition-Metal Electride Y_2C. *Chem. Mater.* **2014**, *26*, 6638–6643.

(26) Zhao, Z.; Zhang, S.; Yu, T.; Xu, H.; Bergara, A.; Yang, G. Predicted Pressure-Induced Superconducting Transition in Electride Li_6P. *Phys. Rev. Lett.* **2019**, *122*, 097002.

(27) Wang, J.; Hanzawa, K.; Hiramatsu, H.; Kim, J.; Umezawa, N.; Iwanaka, K.; Tada, T.; Hosono, H. Exploration of Stable Strontium Phosphide-Based Electrides: Theoretical Structure Prediction and Experimental Validation. *J. Am. Chem. Soc.* **2017**, *139*, 15668–15680.

(28) Chanhom, P.; Fritz, K. E.; Burton, L. A.; Kloppenburg, J.; Filinchuk, Y.; Senyshyn, A.; Wang, M.; Feng, Z.; Insin, N.; Suntivich, J.; et al. Sr_3CrN_3: A New Electride with a Partially Filled D-Shell Transition Metal. *J. Am. Chem. Soc.* **2019**, *141*, 10595–10598.

(29) Miao, M.-s.; Wang, X.-l.; Brgoch, J.; Spera, F.; Jackson, M. G.; Kresse, G.; Lin, H.-q. Anionic Chemistry of Noble Gases: Formation of Mg-NG (NG = Xe, Kr, Ar) Compounds under Pressure. *J. Am. Chem. Soc.* **2015**, *137*, 14122–14128.

(30) Li, P.; Gao, G.; Wang, Y.; Ma, Y. Crystal Structures and Exotic Behavior of Magnesium under Pressure. *J. Phys. Chem. C* **2010**, *114*, 21745–21749.

(31) Dong, X.; Oganov, A. R.; Goncharov, A. F.; Stavrou, E.; Lobanov, S.; Saleh, G.; Qian, G.-R.; Zhu, Q.; Gatti, C.; Deringer, V. L.; et al. A Stable Compound of Helium and Sodium at High Pressure. *Nat. Chem.* **2017**, *9*, 440–445.

(32) Tang, H.; Wan, B.; Gao, B.; Muraba, Y.; Qin, Q.; Yan, B.; Chen, P.; Hu, Q.; Zhang, D.; Wu, L.; et al. Metal-to-Semiconductor Transition and Electronic Dimensionality Reduction of Ca_2N Electride under Pressure. *Adv. Sci.* **2018**, *5*, 1800666.

(33) Rivers, M.; Prakapenka, V.; Kubo, A.; Pullins, C.; Holl, C.; Jacobsen, S. The COMPRES/GSECARS Gas-Loading System for Diamond Anvil Cells at the Advanced Photon Source. *High Pressure Res.* **2008**, *28*, 273–292.

(34) Prescher, C.; Prakapenka, V. B. DIOPTAS: a Program for Reduction of Two-Dimensional X-Ray Diffraction Data and Data Exploration. *High Pressure Res.* **2015**, *35*, 223–230.

(35) Toby, B. H. EXPGUI, a Graphical User Interface for GSAS. *J. Appl. Crystallogr.* **2001**, *34*, 210–213.

https://dx.doi.org/10.1021/acs.jpcc.0c01543
J. Phys. Chem. C 2020, 124, 12213–12219

(36) Oganov, A. R.; Glass, C. W. Crystal Structure Prediction Using Ab Initio Evolutionary Techniques: Principles and Applications. *J. Chem. Phys.* **2006**, *124*, 244704.
(37) Wang, Y.; Lv, J.; Zhu, L.; Ma, Y. CALYPSO: A Method for Crystal Structure Prediction. *Comput. Phys. Commun.* **2012**, *183*, 2063−2070.
(38) Wang, Y.; Lv, J.; Zhu, L.; Ma, Y. Crystal Structure Prediction via Particle-Swarm Optimization. *Phys. Rev. B: Condens. Matter Mater. Phys.* **2010**, *82*, 094116.
(39) Kresse, G.; Furthmüller, J. Efficiency of Ab-Initio Total Energy Calculations for Metals and Semiconductors Using a Plane-Wave Basis Set. *Comput. Mater. Sci.* **1996**, *6*, 15−50.
(40) Perdew, J. P.; Burke, K.; Ernzerhof, M. Generalized Gradient Approximation Made Simple. *Phys. Rev. Lett.* **1996**, *77*, 3865.
(41) Baer, B. J.; Yoo, C.-S.; Cynn, H. X-Ray Induced Luminescence of Solid Argon at High Pressures: A Pressure Probe. *Appl. Phys. Lett.* **2000**, *76*, 3721−3722.
(42) Klotz, S.; Chervin, J.-C.; Munsch, P.; Le Marchand, G. Hydrostatic Limits of 11 Pressure Transmitting Media. *J. Phys. D: Appl. Phys.* **2009**, *42*, 075413.
(43) Zhuang, Y.; Wu, L.; Gao, B.; Cui, Z.; Gou, H.; Zhang, D.; Zhu, S.; Hu, Q. Deviatoric Stress-Induced Quasi-Reconstructive Phase Transition in ZnTe. *J. Mater. Chem.* **2020**, *8*, 3795−3799.
(44) Birch, F. Finite Elastic Strain of Cubic Crystals. *Phys. Rev.* **1947**, *71*, 809−824.
(45) Li, Z.; Yang, J.; Hou, J. G.; Zhu, Q. Is Mayenite without Clathrated Oxygen an Inorganic Electride? *Angew. Chem., Int. Ed.* **2004**, *43*, 6479−6482.
(46) Martinez-Canales, M.; Pickard, C. J.; Needs, R. J. Thermodynamically Stable Phases of Carbon at Multiterapascal Pressures. *Phys. Rev. Lett.* **2012**, *108*, 045704.
(47) Kitano, M.; Inoue, Y.; Ishikawa, H.; Yamagata, K.; Nakao, T.; Tada, T.; Matsuishi, S.; Yokoyama, T.; Hara, M.; Hosono, H. Essential Role of Hydride Ion in Ruthenium-Based Ammonia Synthesis Catalysts. *Chem. Sci.* **2016**, *7*, 4036−4043.
(48) Tada, T.; Takemoto, S.; Matsuishi, S.; Hosono, H. High-Throughput Ab Initio Screening for Two-Dimensional Electride Materials. *Inorg. Chem.* **2014**, *53*, 10347−10358.

https://dx.doi.org/10.1021/acs.jpcc.0c01543
J. Phys. Chem. C 2020, 124, 12213−12219